Molecular Modeling, Affinity Labeling, and Site-Directed Mutagenesis Define the Key Points of Interaction between the Ligand-Binding Domain of the Vitamin D Nuclear Receptor and 1α,25-Dihydroxyvitamin D_3†

Narasimha Swamy,[#,‡] Wenrong Xu,[#,§] Nancy Paz,[‡] Jui-Cheng Hsieh,[||] Mark R. Haussler,[||] George J. Maalouf,[⊥] Scott C. Mohr,[§] and Rahul Ray*[,‡]

Bioorganic Chemistry and Structural Biology Group, Vitamin D Laboratory, Department of Medicine, Boston University School of Medicine, Boston, Massachusetts 02118, Department of Chemistry, Boston University, Boston, Massachusetts 02215, Department of Biochemistry, University of Arizona, College of Medicine, Tucson, Arizona 85724, and Computational Biology, Compaq Computer Corporation, 200 Forest Street, Marlboro, Massachusetts 01752

Received February 2, 2000; Revised Manuscript Received July 24, 2000

ABSTRACT: We have combined molecular modeling and classical structure−function techniques to define the interactions between the ligand-binding domain (LBD) of the vitamin D nuclear receptor (VDR) and its natural ligand, 1α,25-dihydroxyvitamin D_3 [1α,25-$(OH)_2D_3$]. The affinity analogue 1α,25-$(OH)_2D_3$-3-bromoacetate exclusively labeled Cys-288 in the VDR-LBD. Mutation of C288 to glycine abolished this affinity labeling, whereas the VDR-LBD mutants C337G and C369G (other conserved cysteines in the VDR-LBD) were labeled similarly to the wild-type protein. These results revealed that the A-ring 3-OH group docks next to C288 in the binding pocket. We further mutated M284 and W286 (separately creating M284A, M284S, W286A, and W286F) and caused severe loss of ligand binding, indicating the crucial role played by the contiguous segment between M284 and C288. Alignment of the VDR-LBD sequence with the sequences of nuclear receptor LBDs of known 3-D structure positioned M284 and W286 in the presumed β-hairpin of the molecule, thereby identifying it as the region contacting the A-ring of 1α,25-$(OH)_2D_3$. From the multiple sequence alignment, we developed a homologous extension model of the VDR-LBD. The model has a canonical nuclear receptor fold with helices H1−H12 and a single β hairpin but lacks the long insert (residues 161−221) between H2 and H3. We docked the α-conformation of the A-ring into the binding pocket first so as to incorporate the above-noted interacting residues. The model predicts hydrogen bonding contacts between ligand and protein at S237 and D299 as well as at the site of the natural mutation R274L. Mutation of S237 or D299 to alanine largely abolished ligand binding, whereas changing K302, a nonligand-contacting residue, to alanine left binding unaffected. In the "activation" helix 12, the model places V418 closest to the ligand, and, consistent with this prediction, the mutation V418S abolished ligand binding. The studies together have enabled us to identify 1α,25-$(OH)_2D_3$-binding motifs in the ligand-binding pocket of VDR.

Vitamin D receptor (VDR),[1] the nuclear receptor for 1α,25-dihydroxyvitamin D_3 [1α,25-$(OH)_2D_3$], plays a pivotal role in the manifestation of multiple physiological properties of 1α,25-$(OH)_2D_3$, including calcium and phosphorus homeostasis, regulation of the immune response, and modulation of the growth and maturation of normal and malignant cells. 1α,25-$(OH)_2D_3$ binds VDR with high specificity and efficiency, allosterically promoting its heterodimerization with retinoid X receptor (RXR). The liganded dimer interacts with vitamin D response elements (VDREs) in the upstream promoter regions of vitamin D-regulated genes to trigger transcription and translation of the gene products (*1*−*4*). Since binding of 1α,25-$(OH)_2D_3$ to VDR must occur to initiate this cascade of physiological responses, analysis of

† Work was supported in part by Grants DK 44337 and DK 47418 from the National Institute of Diabetes, Digestive and Kidney Diseases of the National Institutes of Health and American Cancer Society Institutional Research Grant, IRG-72-001-24.

* To whom correspondence should be sent. Rahul Ray, Boston University School of Medicine, 80 East Concord St., Boston, MA 02118. Phone: (617) 638-8199. Fax: (617) 638-8194. E-mail: bapi@bu.edu.

[#] These authors contributed equally to this work.

[‡] Department of Medicine, Boston University School of Medicine.

[§] Department of Chemistry, Boston University.

[||] University of Arizona.

[⊥] Compaq Computer Corporation.

[1] Abbreviations: VDR, vitamin D nuclear receptor; hVDR, human VDR; LBD, ligand-binding domain; 1α,25-$(OH)_2D_3$, 1α,25-dihydroxyvitamin D_3; 1α,25-$(OH)_2D_3$-3-BE, 1α,25-dihydroxyvitamin D_3-3β-bromoacetate; VDRE, vitamin D response element; PPAR, peroxisome proliferator-activated receptor γ; PR, progesterone receptor; RAR, retinoic acid receptor γ; hRAR, human RAR; RXR, retinoid X receptor; TR, thyroid hormone receptor α1; GST, glutathione-*S*-transferase; DBP, vitamin D-binding protein; BNPS-skatole, 3-bromo-3-methyl-2-(2-nitrophenylmercapto)-3H-indole; DTT, dithiothreitol; IPTG, isopropyl-thiogalactoside; PMSF, phenylmethanesulfonyl fluoride; RLNE, rat liver nuclear extract; TBS buffer, 50 mM Tris-HCl, 100 mM NaCl, 1.5 mM EDTA, pH 7.4; KTED buffer, 50 mM Tris-HCl, 150 mM NaCl, 300 mM KCl, 1.5 mM EDTA, 10 mM sodium molybdate, and 5 mM DTT, pH 7.4; SDS−PAGE, sodium dodecyl sulfate−polyacrylamide gel electrophoresis; PCR, polymerase chain reaction; PVDF, poly(vinylidene difluoride); DSC, discrimination of protein secondary structure class; PHD, profile-based neural network protein structure prediction; PIMA, pattern-induced multiple alignment; DSSP, database of secondary structure in proteins; RMSD, root-mean-square deviation.

10.1021/bi0002131 CCC: $19.00
Published on Web 09/08/2000

the structure/function aspects of this interaction assumes major significance, especially in light of the fact that more than 500 analogues of 1α,25-$(OH)_2D_3$ have been synthesized and physiological effects of many were analyzed both in vitro and in vivo (*4*).

Sequence comparisons clearly indicate extensive structural homology among the LBDs of members of the nuclear receptor superfamily, including VDR (*5*). This has been corroborated by crystal structure determinations for RXR-α (*6*), retinoic acid receptor γ (RAR) (*7*, *8*), thyroid hormone receptor α1 (TR) (*9*, *10*), estrogen receptor α (ER) (*11*−*13*), progesterone receptor (PR) (*14*), and peroxisome proliferator-activated receptor γ (PPAR) (*15*, *16*). These structures include examples of both the apo and holo (liganded) forms of the ligand-binding domains. Availability of such information invites attempts to describe the mechanism of ligand binding (*17*, *18*) and to construct homology extension models for the LBDs of receptors for which no experimentally determined structure is available (*19*−*22*). Both experimental and modeled structures offer insight into the details of ligand binding that can assist efforts to understand how variations in ligand structure may influence physiological responses. The contrasting behavior of estradiol, the natural ligand for ER, and raloxifene, a synthetic estrogen analogue of great pharmacological interest, provides a case in point (*11*).

Our work has grown out of efforts to define the ligand contact points within the VDR-LDB by means of affinity/photoaffinity labeling techniques. These promised to clarify the interpretation of the effects of mutations (both natural and designed) that had been observed in the VDR-LBD, in particular those resulting in a decrease in hormone binding and/or transcriptional activation (*1*). Without identification of specific attachment points for affinity labels, the mutation data alone could not provide information about the geometry of the ligand-binding pocket, such as the orientation of the bound ligand, nor could it identify the specific contacting parts of the ligand and protein. In the past, our laboratory and others have made several attempts to photoaffinity-label the hormone-binding portion(s) of naturally occurring VDR with very limited success (*23*−*28*). In contrast, we recently showed that 1α,25-dihydroxyvitamin D_3-3β-bromoacetate [1α,25-$(OH)_2D_3$-3-BE], an affinity alkylating derivative of 1α,25-$(OH)_2D_3$, specifically labels the hormone-binding site of natural and recombinant VDR (*29*, *30*). In addition, we were able to locate the affinity label in the C-terminal section (residues 287−427) of full-length human VDR (hVDR) (*31*), i.e., in the LBD (which consists of residues 121−427).

In the present study, we employed a combination of methods to expand upon the affinity-labeling result and develop a much more detailed picture of the interactions between VDR and 1α,25-$(OH)_2D_3$. This included the use of protein chemistry to establish the point of attachment of the affinity label, generation of site-directed mutations to confirm the target location, and construction of a homology extension model to guide further experimentation. Subsequent site-directed mutagenesis experiments largely supported the ligand−protein interactions postulated by the model.

MATERIALS AND METHODS

^{14}C-1α,25-dihydroxyvitamin D_3-3β-bromoacetate [^{14}C-1α,-25-$(OH)_2D_3$-3-BE, specific activity 8.4 mCi/mmol] and 1α,-25-dihydroxy[1β-^{3}H]vitamin D_3 (specific activity 15 Ci/mmol) were synthesized according to published procedures (*30*, *32*). 3-Bromo-3-methyl-2-(2-nitrophenylmercapto)-3H-indole (BNPS-skatole) was purchased from Pierce Chemical Co. (Rockford, IL). pGEX-4T-2 and thrombin were from Pharmacia Biotechnolgies (Piscataway, NJ). Glutathione Sepharose, benzamidine Sepharose, Triton X-100, and reduced glutathione were obtained from Sigma Chemical Co. (St. Louis, MO). ATP and other reagent grade chemicals were purchased from American Bioanalyticals (Natick, MA). Expression and purification of VDR-LBD (105−427) were carried out according to a published procedure (*31*, *33*). Rat liver nuclear extract (RLNE) was prepared according to a published procedure (*34*).

Table 1: Mismatched Oligonucleotide Primers Used for Mutatgenesis[a]

mutant	oligonucleotide
S237A	GACCTGGTCAGTTA***CGC***CATCCAAAAGGTCATT
M284A	TCCACCATGGACGAC***GCC***TCCTGGACCTGT
M284S	ATGGACGAC***AGC***TCCTGGACCTGTGGCAACCAA
W286A	ATGGACGACATGTCC***GCC***ACCTGTGGCAACCAA
W286F	ATGGACGACATGTCC***TTT***ACCTGTGGCAACCAA
D299A	AGGTACCGCGTCAG***TGC***CGTGACCAAAGCCGGA
K302A	GTCAGTGACGTGACC***GCA***GCCGGACACAGCCTG
V418S	AAGCTAACGCCCCTT***TCG***CTCGAAGTGTTTGGC

[a] Bold italics mark the altered codons.

Bacterial Expression of VDR-LBD (105−427) Mutants. Table 1 lists the mutants (other than those derived from Cys; see next paragraph) and the oligonucleotides used to create them by the method of unique-site elimination (U.S.E. mutagenesis kit from Pharmacia Biotech). Changes were confirmed by sequencing. Wild-type and mutant VDR-LBDs (105−427) were cloned into the pGEX-4T2 vector and expressed as C-terminal fusion partners of glutathione-*S*-transferase in an *Escherichia coli* TB1 host. Protein expression was induced by IPTG for 24 h. The cells were subsequently resuspended in the presence of 1 mM PMSF in TBS buffer (50 mM Tris-HCl, 100 mM NaCl, and 1.5 mM EDTA, pH 7.4) and lysed in protease cocktail (0.5 M TBS, 2.5% Triton X-100, 50 mg/mL each of aprotinin, pepstatin, and leupeptin, and 5 mM DTT) with lysozyme (0.1 mg/mL), with freezing, etc. Upon thawing the sample, 10 mM $MgSO_4$ and 300 units of DNase were added to each 40-mL suspension of cell lysate, and after confirmation of DNA cleavage, the broken-cell suspension was sonicated for 30 s and centrifuged, and the lysates were loaded onto a GST-affinity column (equilibrated with TBS/5 mM DTT). The column was washed thoroughly with 50 mM Tris acetate and 5 mM DTT, pH 7.4, buffer, followed by washing with 10 column volumes of the same buffer containing 1 mM ATP and 10 mM $MgSO_4$ to remove contaminating DnaK protein (*33*). The column was finally washed with 50−100 column volumes of 50 mM Tris acetate, pH 7.4, and 5 mM DTT, to remove ATP, and GST-VDR-LBDs were eluted with the same buffer containing 10 mM of reduced glutathione. Purity of the protein samples was determined by SDS−PAGE. GST-fusion proteins were incubated with thrombin (1 unit/100 mg of protein) at 25 °C for 12−14 h, and the digests were purified on a Mono-Q ion-exchange column with 0−500 mM NaCl gradient to separate VDR-LBDs from GST. Purity of the proteins was monitored by SDS−PAGE/Coomasie Blue staining.

Bacterial Expression of Cys Mutants (GST-VDR-LBD). The human VDR expression vectors, pSG5hVDR (*35*), employed earlier to create the plasmids for Cys mutants by site-directed mutagenesis (*36*), were used as templates to obtain oligonucleotide sequences for VDR-LBDs (105−427), which were PCR-amplified, cloned into pGX4T-2 vector, and expressed in *E. coli* as described earlier, except that GST-fusion proteins were not treated with thrombin to remove GST. Thus, the mutants were obtained as N-terminal GST fusion proteins (GST-VDR-LBDs).

Binding Assays of VDR-LBDs with ^{3}H-1α,25-(OH)$_2$D$_3$. These assays were carried out in triplicate with wild-type or mutant VDR-LBDs (50 ng/sample for W286 mutants, 150 ng/sample for M284 mutants, and 300 ng/sample for other mutants), ^{3}H-1α,25-(OH)$_2$D$_3$ (3000 cpm, in 5 μL of ethanol) and rat liver nuclear extract (RLNE, 10 μg of protein/sample) in KTED buffer (50 mM Tris-HCl, 150 mM NaCl, 300 mM KCl, 1.5 mM EDTA, 10 mM sodium molybdate, and 5 mM DTT, pH 7.4). The samples were mixed by vortexing and incubated at 4 °C for 20 min and centrifuged at 1200*g* for 15 min. Supernatant from each sample was mixed with 5 mL of scintillation cocktail and counted in a liquid scintillation counter for radioactivity. Nonspecific binding was determined by carrying out the incubation in the presence of an excess (0.5 μg/sample) of 1α,25-(OH)$_2$D$_3$.

Affinity Labeling of VDR-LBD with ^{14}C-1α,25-(OH)$_2$D$_3$-3-BE and Identification of the Modified Residue by Edman Degradation. VDR-LBD (700 μg, 20 nmol) was treated with 170 000 cpm (20 nmol) of ^{14}C-1α,25-(OH)$_2$D$_3$-3-BE in 50 mM Tris-HCl buffer, pH 7.4, containing 150 mM NaCl, 300 mM KCl, 1.5 mM EDTA, and 5 mM DTT for 14 h at 4 °C. A sample of the reaction was subjected to SDS−PAGE analysis to determine the extent of affinity labeling. The affinity-labeled VDR-LBD was separated from the reaction mixture by desalting on a Superose-HR (30 × 1 cm) gel filtration column equilibrated with 10 mM Tris-HCl buffer, pH 7.4. The affinity-labeled VDR-LBD (10 nmol) was then digested with BNPS-skatole (1 mmol) in 1.0 mL of 70% glacial acetic acid for 72 h at 25 °C. The reaction mixture was dried under vacuum to remove acetic acid, and excess BNPS-skatole was extracted with ethyl acetate. The BNPS-skatole-digested, affinity-labeled VDR-LBD was separated on a 12.5% SDS−PAGE using a Tris-tricine buffer system and blotted onto a PVDF membrane. The protein bands were identified by Coomassie Brilliant Blue staining, and radioactivity was tracked by phosphorimaging. The peptide band containing radioactivity was sequenced on an automated Edman sequencing system. The samples from the reaction chamber in the automated Edman sequencing system were also collected using a fraction collector. Each fraction was mixed with scintillant and counted for radioactivity.

Affinity Labeling of Cys → Gly Mutants (as GST-Fusions) with ^{14}C-1α,25-(OH)$_2$D$_3$-3-BE. A total of 10.0 μg each of GST-VDR-LBDs (wild-type, C288G, C337G, and C369G) were incubated with 5000 cpm of ^{14}C-1α,25-(OH)$_2$D$_3$-3-BE in the presence or absence of 1.0 μg of 1α,25-(OH)$_2$D$_3$ in 50 mM Tris HCl buffer, pH 7.4, containing 150 mM NaCl, 300 mM KCl, 1.5 mM EDTA, and 5 mM DTT for 14 h at 4 °C. The samples were analyzed by 10% SDS−PAGE, and radioactivity was followed by phosphorimaging.

Multialignment of NR-LBD Sequences. The multisequence alignment previously used to construct a model of the human estrogen receptor (*19*) was modified to incorporate the sequences of nuclear receptors with newly determined structures plus the VDR-LBD sequence. VDR secondary structures were assigned accordingly and validated using secondary structure prediction tools PHD and DSC. The long insertion between helix 2 and helix 3 (residues 162−221) was excised since it has little well-predicted secondary structure and no match to similar sequences of determined structure in the Protein Data Bank. Furthermore, most nuclear receptors lack this feature. All known VDR-LBD sequences from different species as retrieved from SwissProt were also aligned to identify more critical parts of the structure on the basis of maximum sequence conservation.

Selection of Modeling Template. The coordinates of hPR-LBD (1A28) (*14*) were adopted with modifications. Helix 1 was extended by four residues in both the amino- and carboxyl-terminal directions by specifying canonical α-helical values for the ϕ,ψ angles to replace those in the reference coordinate set. The coordinates for the long loop between H1 and H3 (residues 143−161) as well as those for the β-sheet structure (residues 283−293) were replaced by the hRAR-LBD (2LBD) (*7*) coordinates for the corresponding aligned segments.

Model Generation and Ligand Docking. Insight II software modules (Molecular Simulations Inc., San Diego, CA) were used to model the VDR sequence onto the selected template according to standard procedures. After creating the VDR structure by substitution of amino acid residues, we carried out several cycles of minimization to generate the tertiary structure of the apoprotein.

Because of the great flexibility of 1α,25-(OH)$_2$D$_3$, we conducted an extensive search of the literature to select the optimum ligand conformation (cf. ref *37*). The key considerations we adopted were (a) an "α-chair" type conformation of the A-ring (*38*) with the α-OH at C-1 in an axial position (which places the C-3 β-OH in equatorial orientation); (b) a ca. 50° dihedral twist around the C-5/C-10 bond; (c) 6-s-trans conformation of the seco-B triene with freedom to rotate around the C-6/C-7 bond; (d) a relatively rigid C/D-ring unit with the D-ring in an "envelope" conformation having C-16 out-of-plane; and (e) a fully extended, freely rotatable side chain.

We docked the ligand by placing it in an initial locus based on the known position of progesterone in the PR-LBD crystal structure, and then rotated and translated it manually by a small amount to relieve a steric clash between the A-ring and helix 5. A few backbone/side-chain atoms of the template were also adjusted to accommodate the whole ligand, without disrupting the overall protein fold. A set of crude models of the complex was constructed and subjected to the Affinity-Grid docking method of Insight II to obtain the best binding structures. This docking method allows flexibility in both the ligand and the ligand-binding pocket residues of the receptor. In addition, distance-based, hydrogen-bond penalty terms were added in the energy calculation to constrain the A-ring hydroxyl groups to their hydrogen bond partners (S237, R274, S275) during the Monte Carlo minimization. Hydrogen bond partners for the two hydroxyl groups on the A-ring were selected on the basis of (a) proximity in the preliminarily docked structure, (b) comparison with ligand-binding positions in other nuclear receptors of determined structure, and (c) review of all available mutation data on

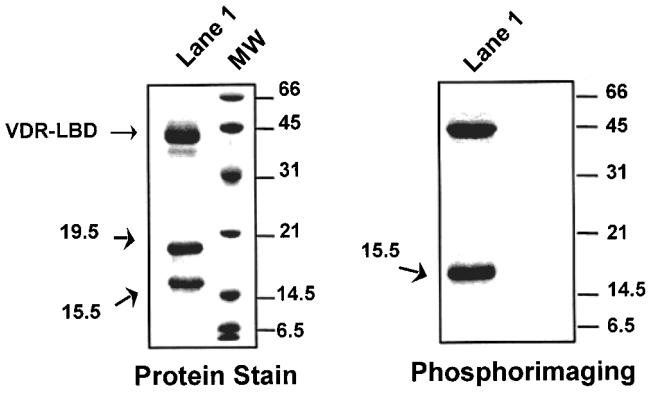

FIGURE 1: BNPS-skatole cleavage of VDR-LBD, affinity-alkylated with ^{14}C-1α,25-$(OH)_2D_3$-3-BE. A VDR-LBD sample, affinity-labeled with ^{14}C-1α,25-$(OH)_2D_3$-3-BE, was digested with BNPS-skatole in 70% acetic acid at 25 °C for 72 h. After the removal of the solvent and extraction of the excess of BNPS-skatole, the sample was analyzed by SDS−PAGE on a 10% gel with standard MW markers running alongside. Protein bands were visualized with Coomasie Brilliant Blue staining, and radioactivity was identified by phosphorimaging. Lane 1: BNPS-skatole digest. Positions of standard MW marker proteins are designated at the right. The 45-kDa band represents VDR-LBD not cleaved by BNPS-skatole.

VDR. The 20 best-docked structures were examined and screened for possible hydrogen bond partners of the 25-hydroxyl group as well as for compliance with the biological data. One complex had D299 and the 25-OH in proximity to each other and did not change significantly when subjected to unconstrained molecular dynamics. We selected this model structure as our guide for mutational studies.

RESULTS AND DISCUSSION

Determination of the three-dimensional architecture of VDR-LBD and identification of amino acid residues that are important for orienting, docking, and binding the hormone and its biologically important synthetic analogues are crucial for the elucidation of the complex genomic mechanism mediated by 1α,25-$(OH)_2D_3$ as well as for developing 1α,25-$(OH)_2D_3$-based therapeutic agents. During the past several years, our laboratory has been involved in probing the 1α,25-$(OH)_2D_3$-binding pocket of VDR by affinity and photoaffinity labeling techniques, and in this effort we have recently developed 1α,25-$(OH)_2D_3$-3-BE as an efficient affinity-alkylating agent specific for VDR-LBD (*29*, *30*). We have also exploited the fact that human VDR (hVDR) contains a single Trp residue at position 286 to dissect the protein into two halves using BNPS-skatole, a reagent that cleaves peptide bonds on the C-terminal side of Trp residues under acidic conditions (*39*). Recently, we employed this method to cleave ^{14}C-1α,25-$(OH)_2D_3$-3-BE-labeled hVDR with BNPS-skatole and located the affinity label exclusively in the C-terminal domain (287−427) of VDR (*31*).

Identification of C288 as the Residue that is Affinity-Alkylated by ^{14}C 1α,25-$(OH)_2D_3$-3-BE. In the present investigation, we first focused our attention on identifying the specific amino acid residue/residues modified by 1α,25-$(OH)_2D_3$-3-BE. BNPS-skatole digestion of VDR-LBD, affinity-labeled with ^{14}C-1α,25-$(OH)_2D_3$-3-BE, produced two Coomasie Blue-stained peptide bands with M_r of 19.5 and 15.5 kDa (the M_r 45 kDa band represents the undigested protein), as shown in lane 1, Figure 1 (left panel). Phosphorimaging of the gel showed that radioactivity was associated only with the smaller of the two peptides and the band corresponding to undigested protein (lane 1, Figure 1, right panel).

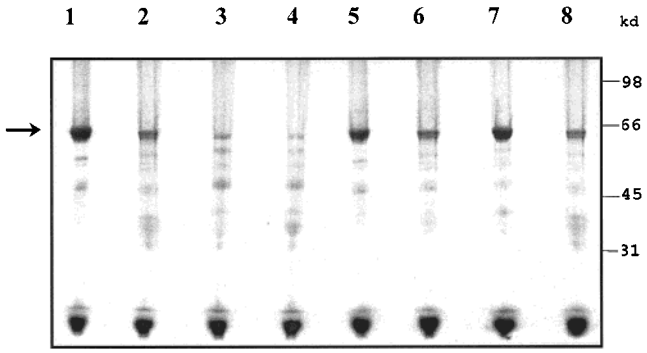

FIGURE 2: Affinity-labeling studies of the wild-type GST-VDR-LBD and Cys-mutants with ^{14}C-1α,25-$(OH)_2D_3$-3-BE. GST-VDR-LBDs (10.0 μg each of wild type, C288G, C337G, and C369G) were incubated with 5000 cpm of ^{14}C-1α,25-$(OH)_2D_3$-3-BE in the presence or absence of 1.0 μg of 1α,25-$(OH)_2D_3$ for 14 h at 4 °C. After the incubation, the samples were analyzed by 10% SDS−PAGE, and radioactivity was followed by phosphorimaging. Positions of the standard MW marker proteins are shown at the right. The arrow at the left designates the position of GST-VDR-LBD. Lane 1: wild-type GST-VDR-LBD + ^{14}C-1α,25-$(OH)_2D_3$-3-BE; lane 2: wild-type GST-VDR-LBD + ^{14}C-1α,25-$(OH)_2D_3$-3-BE + 1α,25-$(OH)_2D_3$ (excess); lane 3: GST-C288G-LBD + ^{14}C-1α,25-$(OH)_2D_3$-3-BE; lane 4: GST-C288G-LBD + ^{14}C-1α,25-$(OH)_2D_3$-3-BE + 1α,25-$(OH)_2D_3$ (excess); lane 5: GST-C337G-LBD + ^{14}C-1α,25-$(OH)_2D_3$-3-BE; lane 6: GST-C337G-LBD + ^{14}C-1α,25-$(OH)_2D_3$-3-BE + 1α,25-$(OH)_2D_3$ (excess); lane 7: GST-C369G-LBD + ^{14}C-1α,25-$(OH)_2D_3$-3-BE; lane 8: GST-C369G-LBD + ^{14}C-1α,25-$(OH)_2D_3$-3-BE + 1α,25-$(OH)_2D_3$ (excess).

Partial N-terminal amino acid sequencing of the 15.5 kDa band revealed the sequence TXGNQDYKYR. This matches the VDR segment corresponding to residues 287−296, but the second residue, C288, was undetectable. The identity of this "missing" residue was ascertained by collecting fractions from each reaction cycle in the Edman degradation and determining their radioactivity. Most of the radioactivity was associated with the second (missing) residue, indicating that the C288 is the amino acid residue modified by ^{14}C-1α,25-$(OH)_2D_3$-3-BE.

The above results were further confirmed by the C288G mutation. We predicted that since replacement of Cys with Gly would remove the nucleophilic sulfhydryl (-SH) group that is required to form a covalent bond with the carbon atom bearing the bromide (Br^-) leaving group in the affinity reagent, it should obliterate labeling. As shown in Figure 2, lanes 3 and 4, the GST-VDR-LBD C288G mutant was not labeled by ^{14}C-1α,25-$(OH)_2D_3$-3-BE, either in the absence (lane 3) or in the presence (lane 4) of an excess of 1α,25-$(OH)_2D_3$, while the wild-type (GST-VDR-LBD) was specifically labeled (lane 1: without 1α,25-$(OH)_2D_3$, lane 2: with an excess of 1α,25-$(OH)_2D_3$) by the affinity label). These results confirmed that ^{14}C-1α,25-$(OH)_2D_3$-3-BE affinity-alkylated C288 in the VDR-LBD and that structural integrity of C288 was essential for such covalent modification. It should be noted that the labeling in lanes containing an excess of 1α,25-$(OH)_2D_3$ was significantly reduced but not eliminated completely. That is to be expected, because a small but significant amount of labeled VDR will always contaminate unlabeled VDR due to the kinetic nature of the labeling process.

Demonstration that C288 is the Only Cys Residue in VDR-LBD Affinity-Labeled by ^{14}C-1α,25-(OH)$_2$D$_3$-3-BE. Cysteine residues play important roles in the structural and functional integrity of proteins, and for steroid hormone receptors in particular, certain cysteines are essential for high-affinity ligand binding (*40*). In 1979, Wecksler et al. (*41*) treated rat intestinal cytosol, containing VDR, with iodoacetamide and *N*-ethylmaleimide, well-known cysteine-modifying agents, and observed that 1α,25-(OH)$_2$D$_3$ binding was adversely affected, suggesting that cysteine residues play a crucial role in hormone binding. Coty also made related observations using cysteine-modifying organomercurials (*42*). Similarly, it was observed that the DNA-binding domain of VDR contains essential Cys residues that are modified by *p*-chloromercuribenzenesulfonate (*43*). The conservation of C288, C337, and C369 in human, bovine, rat, mouse, chicken, Japanese quail, and *Xenopus* VDR underscores the essential nature of these residues (*44*−*47*).

Nakajima et al. recently reported that hormone binding was seriously compromised by the C288G mutation, while C337G and C369G mutants showed only moderate impairment (*36*). To better define the behavior of C337 and C369 with respect to the affinty label, we expressed the LBDs of GST-C337G and GST-C369G mutants and reacted them with ^{14}C-1α,25-(OH)$_2$D$_3$-3-BE. As shown in Figure 2, while the wild-type protein and the GST-C337G and GST-C369G mutant proteins were labeled by ^{14}C-1α,25-(OH)$_2$D$_3$-3-BE in the absence of any 1α,25-(OH)$_2$D$_3$ (lanes 1, 5, and 7, respectively), there was significant reduction in labeling in the presence of an excess of 1α,25-(OH)$_2$D$_3$ (lanes 2, 6, and 8). These results indicated that ^{14}C-1α,25-(OH)$_2$D$_3$-3-BE covalently modified C337G and C369G mutants similar to wild type. In contrast, the C288G mutant protein was not labeled in the presence or absence of 1α,25-(OH)$_2$D$_3$ (lanes 3 and 4), indicating that the affinity alkylation process only involves C288.

Identification of C288 as the sole residue in the VDR-LBD covalently modified by the affinity label confirms the results of point-mutation studies showing the critical nature of this residue for hormone binding (*36*). Moreover, the affinity-labeling process demands that C288 be positioned within bonding distance of the bromoacetate group of LBD-bound ^{14}C-1α,25-(OH)$_2$D$_3$-3-BE because covalent labeling requires such a juxtaposition (Figure 3, panel A). Finally, and most significantly, since the chemically modified portion of ^{14}C-1α,25-(OH)$_2$D$_3$-3-BE is the 3β-hydroxyl group, these results also indicate that in the 1α,25-(OH)$_2$D$_3$/receptor complex, C288 lies close to the 3-OH, either contacting the ligand directly or stabilizing the local conformation of the binding pocket. This could explain the impairment of hormone binding by its mutation to glycine.

The high fidelity of labeling by 1α,25-(OH)$_2$D$_3$-3-BE contrasts sharply with similar studies on the LBD of the estrogen receptor (*48*). For example, Aliau et al. (*49*) recently demonstrated that a quadruple mutant of ER, in which all four cysteine residues (381, 417, 447, and 530) were mutated to alanine, displayed very little labeling by 17α-haloacetamidoalkyl-estradiols (where halo = bromo or iodo; and alkyl = methyl, ethyl, or propyl; cf. Figure 3, panel B). On the other hand, each of the four single Cys → Ala mutants was labeled as efficiently as the wild-type ER. These results indicate that in this system an affinity label can simply "slide"

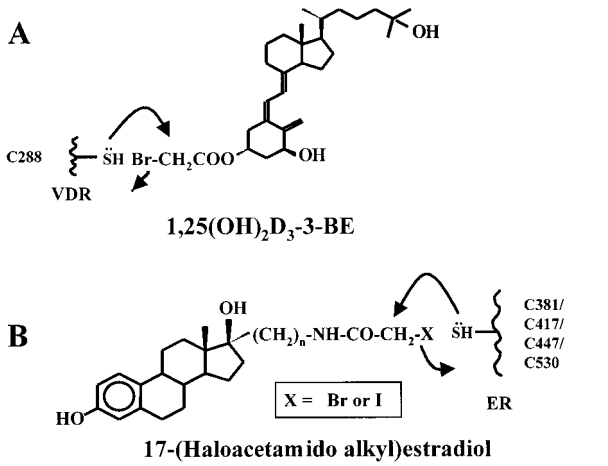

FIGURE 3: Schematic mechanisms of the affinity-alkylation reactions of Cys residues in the LBDs of (A) VDR and (B) ER by 1α,25-(OH)$_2$D$_3$-3-BE and 17α-(haloacetamidoalkyl)-estradiols, respectively.

from one Cys to the other inside the comparatively large binding pocket. If a specific Cys is not available (mutated) the alkylating agent reorients so as to react with one of the remaining three Cys residues.[2] Clearly, VDR represents a different type of situation, at least insofar as reaction with 1α,25-(OH)$_2$D$_3$-3-BE is concerned. Our data clearly show that only one of the three cysteines involved in hormone binding in the LBD reacts with the affinity labeling reagent, indicating that VDR has a very tight binding pocket in the vicinity of the A-ring. As described below, molecular modeling also suggests tight receptor/ligand interaction in the vicinity of C288.

Role of W286 in 1α,25-(OH)$_2$D$_3$ Binding. The conjugated triene moiety, attached to the A-ring of 1α,25-(OH)$_2$D$_3$, represents a unique structural feature, a six-center (acyclic) delocalized π-electron system, which sets this molecule apart from the other steroid hormones. Differential recognition of these ligand molecules by their cognate receptor LBDs must of necessity exploit such singular features. We hypothesized that if the 3-OH group of 1α,25-(OH)$_2$D$_3$ is positioned close to C288 (as the evidence described in the previous section shows), a neighboring amino acid residue with a large delocalized π-electron cloud might interact with the triene part of 1α,25-(OH)$_2$D$_3$ and stabilize the hormone binding. As mentioned earlier, human VDR contains a single Trp (W286), which is next to C288 and contains a large delocalized, polarizable π-electron cloud. Moreover, sequence−structure alignment of the VDR-LBD amino acid sequence with the corresponding sequences of NR-LBDs of known three-dimensional structure places W286 and C288 in a β-hairpin (see below), and since they are two residues apart, their side chains project in approximately the same spatial direction (i.e., toward the ligand).

To assess the role of W286 in hormone binding, we changed this Trp to Ala and Phe by site-directed mutagenesis and determined specific ^{3}H-1α,25-(OH)$_2$D$_3$-binding capabilities of these mutants as compared with the wild type. As shown in Figure 4, panel A, W286A and W286F mutations

[2] A similar case of "tumbling" inside the binding pocket was reported for estradiol-17β-dehydrogenase, where estradiol-17-bromoacetate and estradiol-3-bromoacetate covalently labeled the same His residue in the active site of the enzyme (*50*).

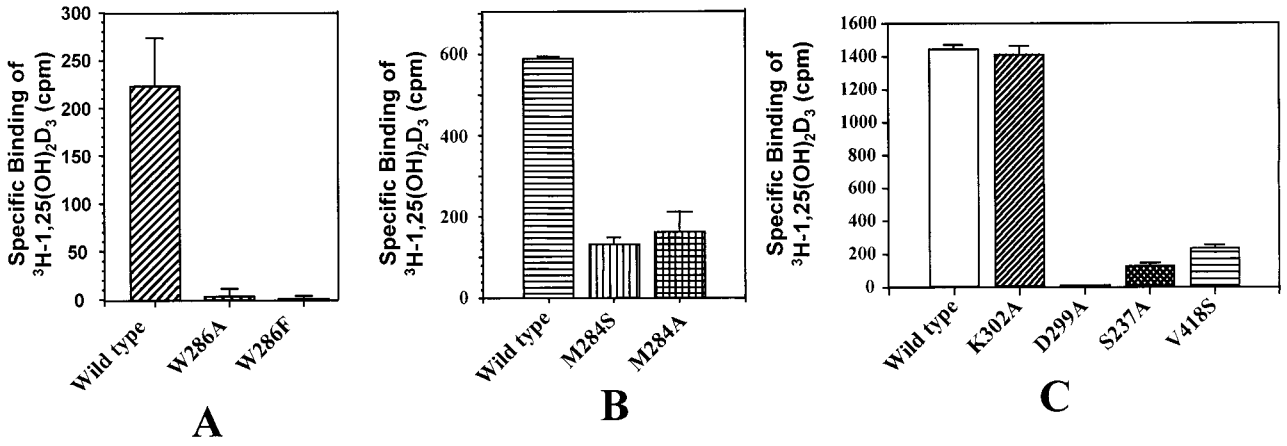

FIGURE 4: (A) Binding assays of wild-type VDR-LBD and W286 site-directed mutants with ^{3}H-1α,25-(OH)$_2$D$_3$. A solution of protein (50 ng/sample), ^{3}H-1α,25-(OH)$_2$D$_3$ (15 Ci/mmol, 3000 cpm, 0.02 fmol), and RLNE (10 μg of protein/sample) in KTED buffer were incubated at 4 ° C for 20 min with or without an excess of 1α,25-(OH)$_2$D$_3$ (0.5 μg/sample), and centrifuged at 1200*g* for 15 min. Supernatant from each sample was mixed with scintillation cocktail and counted. Radioactivity (in cpm) associated with each sample incubated with 1α,25-(OH)$_2$D$_3$ was subtracted from the corresponding sample without 1α,25-(OH)$_2$D$_3$ to calculate specific binding. Assays for each protein sample were carried out in triplicate and error bars designate the standard deviation. (B) Binding assays of wild-type VDR-LBD and M284 site-directed mutants with ^{3}H-1α,25-(OH)$_2$D$_3$. Protocol exactly as in panel A except that samples each contained 150 ng of protein. (C) Binding assays with ^{3}H-1α,25-(OH)$_2$D$_3$ of wild-type VDR-LBD and site-directed mutants selected on the basis of modeling results. Protocol exactly as in panel A except that samples each contained 300 ng of protein.

both resulted in >90% loss of hormone binding. Furthermore, this result underscored the possible stabilizing interaction between this Trp residue and the triene part of 1α,25-(OH)$_2$D$_3$, a result subsequently borne out by molecular modeling studies. It is noteworthy that even replacement of Trp with Phe—which, although smaller, still has a π-electron cloud—was not sufficient to retain appreciable ligand binding. Interestingly, chemical modification (*51*) or site-directed mutagenesis (*52*) of W145, the single Trp in human vitamin D-binding protein (DBP), also resulted in a complete loss of 25-hydroxyvitamin-D$_3$ binding, indicating possible similarities in the vitamin D sterol-binding pockets of DBP and VDR, otherwise unrelated proteins (*53*−*56*).

Role of M284 in 1α,25-(OH)$_2$D$_3$ Binding. Two positions N-terminal of W286 lies a methionine residue (M284), which according to our alignment (cf. Figure 5) should also have an inward-facing side chain along the β-strand that contains C288. Met residues, with their comparatively large, apolar mercaptomethyl side chains, usually engage in nonbonding hydrophobic interactions with ligands. For example, Met residues have been shown to be present in the hydrophobic ligand-binding cavities of ER, PR, TR, and RAR (*57*). Thus, we investigated the potential role of M284 in VDR hormone binding by site-directed mutagenesis of Met to Ala or Ser, followed by ^{3}H-1α,25-(OH)$_2$D$_3$-binding analysis of these mutant proteins. Results of these assays, shown in Figure 4, panel B, demonstrated that there was 78 and 70% loss of ^{3}H-1α,25-(OH)$_2$D$_3$ binding by M284S and M284A mutants, respectively, as compared to the wild type. Thus, collectively these results strongly suggested that in addition to C288 and W286, M284 is involved in hormone binding in a significant way, possibly providing nonbonding, hydrophobic interaction.

Description of a Homology Extension Model of VDR. In the absence of an X-ray crystallographic structural model of the VDR-LBD, we developed a homology model as described in Materials and Methods. Our objective was to elucidate the factors governing the interactions between the VDR-LBD and its natural and synthetic ligands. The discovery of the key position of C288 vis-á-vis the A-ring of bound 1α,25-(OH)$_2$D$_3$ provided crucial information to establish a correct ligand-docking position. The earlier model of Wurtz et al. (*20*) clearly erred in this regard. We chose a hybrid template mainly based on the structure of PR to develop the homology model. Although, on the basis of sequence comparison, the thyroid hormone receptor probably would make a better template for modeling VDR, the structural coordinates of the X-ray crystallographic model of TR only became publicly available after we had completed our work.[3]

Figure 5 displays the sequence/structure alignment used for modeling. Note the position of the 60-residue-long insertion (162−221) that we excised because of the absence of any structural information on which to base a model. Since none of the other nuclear receptors has such a large loop in this position and all of the canonical LBD secondary structural elements could be well-aligned for the rest of the VDR-LBD, omission of this portion of the sequence would almost certainly have had no major effect on the structure of the ligand-binding pocket. The function of this loop in the activity of VDR remains completely mysterious, and its great sequence variability from species to species suggests a relatively unimportant role, with the exception of serine residues that are potential targets for phosphorylation.[4]

Figure 6, panel A depicts the overall tertiary structure of the VDR−LBD with a ribbon diagram; it matches well the folds of the nuclear receptors of known structure (*57*). In Figure 6, panel B, we have cut away helix H12 to reveal the ligand/protein interactions. Note the positions of hydrogen bonding groups (details summarized in Table 2) and the hydrophobic contact of W286 with the ligand. As predicted,

[3] Presented at the First International Conference on Chemistry and Biology of Vitamin D Analogs held at Rhode Island Hospital, Providence, RI, September 26−28, 1999.

[4] An alignment of VDR sequences from seven species (human, bovine, rat, mouse, chicken, Japanese quail, and *Xenopus*) indicates 38 out of 60 positions with significant differences, though there are 8 positions (5 of them serine residues), which are absolutely conserved (data not shown).

FIGURE 5: Sequence−structure alignment for VDR homology model. The sequence of human VDR (vdr, shaded) has been aligned with the sequences of six nuclear receptors of known structure: human estrogen receptor (er), human progesterone receptor (pr), rat thyroid hormone receptor (tr), human peroxisome proliferator-activated receptor (ppar), human retinoic acid receptor (rar), and human retinoid X receptor (rxr). Decadic residue positions are numbered for the VDR sequence (aligned with the middle digit); sequence positions corresponding to the last amino acid in each row are given in the column at the right. The original multialignment was performed with PIMA (*19*), and then adjusted manually with inspection of the secondary structure alignments. Hyphens indicate gaps. Asterisks in the VDR sequence show the location of the large insertion (residues 162−221), which has not been included in the modeled structures. The VDR sequence shown begins at the start of the LBD (residue 121). α-Helices are marked by a single underline and have been identified by the program DSSP except in the case of the thyroid hormone receptor whose coordinates were not publicly available. Secondary structure boundaries in that case have been taken from Figure 1 in Wagner et al. (*9*). *β*-Strands identified by DSSP (except in the case of tr) are doubly underlined. Helices and strands are numbered according to the original scheme used for RXR (*6*). Residues involved in the secondary structural elements of VDR as predicted by the model are given in boldface for convenient reference. The PR sequence has been truncated four residues short of its C terminus to save space (it concludes as ...FHKK).

this large, aromatic residue interacts with the triene part of 1α,25-$(OH)_2D_3$. Figure 6, panel C, shows the "back" of the binding pocket where the same interactions can be seen (in this case none of the structure has been deleted). M288 (shown in blue) functions to provide hydrophobic contacts that buttress the W286/ligand interaction.

In Figure 6, panel D, we show a "side" view of the VDR-LBD with the cysteines accentuated by space-filling display. Clearly, C288 contacts the ligand (that can also be seen in Figure 6, panel C), but none of the others are close to it. (Two of the eight Cys residues of the LBD fall in the 60-residue loop segment that we excised before building the model; its position is indicated by the black stick representation of D161 in Figure 6, panel D.) The molecular modeling results explain our affinity labeling data (described above) by the tight binding of the A-ring of 1α,25-$(OH)_2D_3$ (which makes three hydrogen bonds to the protein, cf. Table 2), by the close positioning of C288 to the ligand and by the disposition of the unlabeled C residues at positions remote from the binding pocket.[5]

Site-Directed Mutagenesis Confirming Features Predicted by the Homology Model. We constructed four additional site-directed mutants to test the interactions predicted by the homology model: S237A, D299A, K302A, and V418S. In the model, S237 is the sole hydrogen bonding partner for the 3-OH group of 1α,25-$(OH)_2D_3$, and since deletion of this hydroxyl group on the ligand greatly weakens binding (*4*), we wanted to confirm the report that the complementary S237A mutation also does so (*58*), consistent with the presence of the postulated hydrogen bond. The result presented in Figure 4, panel C, shows that this is indeed the case: S237A showed 90% loss in binding of the hormone. The hydrogen bonding partner for the 25-OH group of 1α,25-$(OH)_2D_3$ predicted from model I is D299, and the D299A mutation completely abolished hormone binding (Figure 4, panel C). Although the model suggests a salt link between D299 and K302, mutation of the latter to alanine has no effect

[5] The atomic coordinates of this model (I) are available in downloadable pdb-format at http://www.vdr.bu.edu.

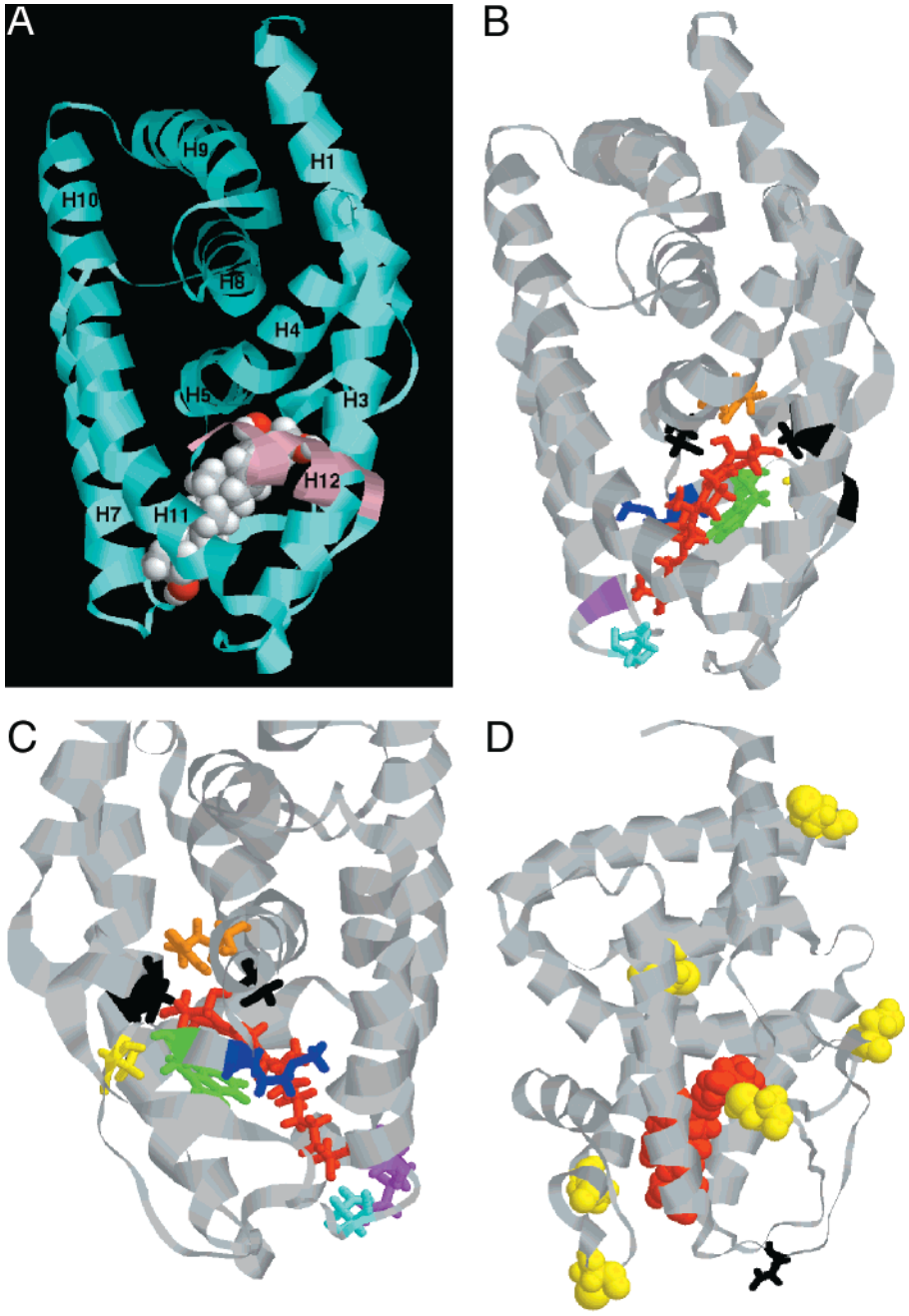

FIGURE 6: Features of VDR-LBD homology model I: (A) Overall view of the 3° structure in ribbon representation. The CPK-colored, space-filling image depicts bound 1α,25-$(OH)_2D_3$, and helix 12 is shown in pink. (B) Cut-away view (helix 12 truncated at P416) of the ligand-binding pocket from the "front" with key amino acid residues shown as stick figures, S237 and S275 in black, R274 in orange, M284 in blue, W286 in green, C288 in yellow, and D299 in cyan. 1α,25-$(OH)_2D_3$ is shown in stick models colored red. The ribbon positions of K302 and P416 are colored magenta and black, respectively. (C) A "back" view of the ligand-binding pocket (seen through the β-hairpin) showing key residues color-coded as in panel B. (D) Ribbon diagram of the VDR-LBD model with all cysteine residues shown in yellow, space-filling representations. C288 nearly touches the ligand (shown as a red, space-filling model); C369 is at the top right of the image, and C337 is obscured by helix 3 in the upper half of the molecule. The black segment in the loop at the bottom right marks the position of D161 that immediately precedes the 60-residue insertion that was omitted from the modeling (see text for details).

Table 2: Predicted Hydrogen Bonding Interactions

ligand group	VDR hydrogen bonding residue	residue role
C-1 -OH	R274	donor
C-1 -OH	S275	acceptor
C-3 -OH	S237	acceptor
C-25 -OH	D299	acceptor

on binding. Conceivably, the two charged residues interact, but this has no significance for the binding of ligand, or the position of the lysine is misleading because we omitted solvent water from the model calculations. Among the inward-facing, hydrophobic residues of helix H12, the model places V418 closest to 1α,25-$(OH)_2D_3$, and again the mutagenesis result (for V418S, cf. Figure 4, panel C) supports this predicted interaction: V418S showed 85% loss in binding of the hormone.

After completion of this work and submission of the manuscript, the paper by Rochel et al. (*59*) describing the crystal structure of a liganded, engineered VDR-LDB appeared. The tertiary fold of the model presented here agrees

reasonably well with the crystal structure (backbone RMSD for helices: 2.5 Å). The greatest difference in the protein structure occurs in the β-hairpin, which lies significantly further back (away from H12) in the crystal structure than it does in our model. The ligand orientation in the model, while having overall similarity, differs in detail from that in the crystal structure, particularly with respect to the placement of the long side chain of the 25-OH group. Two of four identified hydrogen bond partners of the A-ring hydroxyl groups (S237 and R274) have similar functions in the model and the crystal structure. All of the mutation results reported in this paper can be readily explained by reference to side chain/ligand interactions seen in the crystal structure with the exception of D299A. In that case, however, we note that D299 may help stabilize a cluster of positively charged residues (R158, K294, R296, and K302) that sit in the vicinity of the β-hairpin. The hairpin conformation is obviously critical for ligand binding, as seen, for example, from the consequences of mutations C288G, M284A, and M284S. The distance between the sulfur of C288 and the oxygen at position 3 of 1α,25-$(OH)_2D_3$ in the crystal structure is 4.67 Å, consistent with the affinity alkylation result we have reported for 1α,25-$(OH)_2D_3$-3-bromoacetate.

CONCLUSIONS

The combination of chemical modification by an affinity reagent, site-directed mutagenesis, and detailed modeling with a full sequence/structure multialignment allowed us to draw the following conclusions: (i) Assuming the "mousetrap" model for NR ligand binding (*17*, *18*) the A-ring of 1α,25-$(OH)_2D_3$ inserts into the ligand-binding pocket first. This leaves the flexible side-chain projecting toward H12 in the liganded receptor. (ii) The 3-OH group of 1α,25-$(OH)_2D_3$ is adjacent to C288. (iii) Residues S237, R274, and S275 are the likely hydrogen bonding partners of the A-ring's hydroxyl groups. This tight binding probably constrains the A-ring into a single chair conformer. (iv) Residue W286 makes direct hydrophobic contact with 1α,25-$(OH)_2D_3$, probably via the triene moiety, and M284 contributes to a hydrophobic cluster in the vicinity of W286. (v) The flexible side chain of 1α,25-$(OH)_2D_3$ has multiple conformational states available in the ligand-binding pocket and interacts strongly with D299 and V418.

The homologous extension model constitutes one approximation of hormone binding in the VDR-LBD. The important point, however, is that the interplay between experiment and modeling in this case has enabled a much clearer picture of the liganded VDR-LBD to emerge prior to the availability of a crystal structure. A recent study by Yamamoto et al. (*60*) published after completion of this work, takes a similar approach, although with results that differ in detail from ours. As the production of genome sequence data far outpaces the capacity to determine structures experimentally, this paradigm will become increasingly valuable. It is also noteworthy that even with a determined X-ray structure for liganded VDR-LBD, modeling of the complexes formed with its very numerous artificial ligands will play an important role in advancing the vitamin D field.

ACKNOWLEDGMENT

We thank Professor Temple Smith for encouragement and helpful discussions.

REFERENCES

1. Haussler, M. R., Whitfield, G. K., Haussler, C. A., Hsieh, J., Thompson, P. D., Selznick, S. H., Dominguez, C. E., and Jurutka, P. W. (1998) *J. Bone Min. Res. 13*, 325−349.
2. Jones, G., Strugnell, S. A., and DeLuca, H. F. (1998) *Physiol. Rev. 78*, 1193−1231.
3. Norman, A. W. (1998) *J. Bone Min. Res. 13*, 1360−1369.
4. Bouillon, R., Okamura, W. H., and Norman, A. W. (1995) *Endocr. Rev. 16*, 200−257.
5. Laudet, V., Hänni, C., Coll, J., Catzeflis, F., and Stéhelin, D. (1992) *EMBO J. 11*, 1003−1013.
6. Bourguet, W., Ruff, M., Chambon, P., Gronemeyer, H., and Moras, D. (1995) *Nature 375*, 377−382.
7. Renaud, J.-P., Rochel, N., Ruff, M., Vivat, V., Chambon, P., Gronemeyer, H., and Moras, D. (1995) *Nature 378*, 681−689.
8. Klaholz, B. P., Renaud, J.-P., Mitschler, A., Zusi, C., Chambon, P., Gronemeyer, H., and Moras, D. (1998) *Nat. Struct. Biol. 5*, 99−102.
9. Wagner, R. L., Apriletti, J. W., McGrath, M. E., West, B. L., Baxter, J. D., and Fletterick, R. J. (1995) *Nature 378*, 690−697.
10. Darimont, B. D., Wagner, R. L., Apriletti, J. W., Stallcup, M. R., Kushner, P. J., Baxter, J. D., Fletterick, R. J., and Yamamoto, K. R. (1998) *Genes Dev. 12*, 3343−3356.
11. Brzozowski, A. M., Pike, A. C. W., Dauter, Z., Hubbard, R. E., Bonn, T., Engström, O., Öhman, L., Greene, G. L., Gustafsson, J.-A., and Carlquist, M. (1997) *Nature 389*, 753−757.
12. Tanenbaum, D. M., Wang, Y., Williams, S. P., and Sigler, P. B. (1998) *Proc. Natl. Acad. Sci. U.S.A. 95*, 5998−6003.
13. Shiau, A. K., Barstad, D., Loria, P. M., Cheng, L., Kushner, P. J., Agard, D. A., and Greene, G. L. (1998) *Cell 95*, 927−937.
14. Williams, S. P., and Sigler, P. B. (1998) *Nature 393*, 392−396.
15. Nolte, R. T., Wisely, G. B., Westin, S., Cobb, J. E., Lambert, M. H., Kurokawa, R., Rosenfeld, M. G., Willson, T. M., Glass, C. K., and Milburn, M. V. (1998) *Nature 395*, 137−143.
16. Uppenberg, J., Svenson, C., Jaki, M., Bertilsson, G., Jendberg, L., and Berkenstam, A. (1998) *J. Biol. Chem. 273*, 31108−31112.
17. Wurtz, J.-M., Bourguet, W., Renaud, J.-P., Vivat, V., Chambon, P., Moras, D., and Gronemeyer, H. (1996) *Nature Struct. Biol. 3*, 87−94.
18. Blondel, A., Renaud, J.-P., Fischer, S., Moras, D., and Karplus, M. (1999) *J. Mol. Biol. 291*, 101−115.
19. Maalouf, G. J., Xu, W., Smith, T. F., and Mohr, S. C. (1998) *J. Biomolec. Struct. Dyn. 15*, 841−851.
20. Wurtz, J.-M., Guillot, B., and Moras, D. (1997) in *Vitamin D: Chemistry, Biology and Clinical Applications of the Steroid Hormone* (Norman, A. W., Bouillon, R., and Thomasset, Eds.), pp 165−172, University of California, Riverside, CA.
21. Norman, A. W., Adams, D. M., Collins, E. D., Okamura, W. H., and Fletterick, R. J. (1999) *J. Cell. Biochem. 74*, 323−333.
22. Yamamoto, K., Masuno, H., Choi, M., Nakashima, K., Taga, T., Ooizumi, H., Umesono, K., Sicinska, W., VanHooke, J., DeLuca, H. F., and Yamada, S. (2000) *Proc. Natl. Acad. Sci. U.S.A., 97*, 1467−1472.
23. Ray, R., Holick, S. A., and Holick, M. F. (1985) *J. Chem. Soc. Chem. Commun.* 702−703.
24. Ray, R., Rose, S. R., Holick, S. A., and Holick, M. F. (1985) *Biochem. Biophys. Res. Commun. 132*, 198−203.
25. Ray, R., and Holick, M. F. (1988) *Steroids 51*, 623−630.
26. Ray, R., Ray, S., and Holick, M. F. (1993) *Steroids 58*, 462−465.
27. Brown, T. A., and DeLuca, H. F. (1991) *Biochim. Biophys. Acta 1073*, 324−328.
28. Roy, A., and Ray, R. (1995) *Steroids 60*, 530−533.
29. Ray, R., Ray, S., and Holick, M. F. (1994) *Bioorg. Chem. 22*, 276−283.
30. Ray, R., Swamy, N., MacDonald, P. N., Ray, S., Haussler, M. R., and Holick, M. F. (1996) *J. Biol. Chem. 271*, 2012−2017.
31. Swamy, N., Kounine, M., and Ray, R. (1997) *Arch. Biochem. Biophys. 348*, 91−95.

32. Ray, R., and Holick, M. F. (1997) *Methods Enzymol. 282*, 157−164.
33. Swamy, N., Mohr, S. C., Xu, W., and Ray, R. (1999) *Arch. Biochem. Biophys. 363*, 219−226.
34. Nakajima, S., Hsieh, J.-C., MacDonald, P. N., Haussler, C. A., Galligan, M. A., Jurutka, P. W., and Haussler, M. R. (1993) *Biochem. Biophys. Res. Commun. 197*, 478−485.
35. Hsieh, J.-C., Jurutka, P. W., Galligan, M. A., Terpening, C. M., Haussler, C. A., Samuels, D. S., Shimizu, Y., Shimizu, N., and Haussler, M. R. (1991) *Proc. Natl. Acad. Sci. U.S.A. 88*, 9315−9319.
36. Nakajima, S., Hsieh, J.-C., Jurutka, P. W., Galligan, M. A., Haussler, C. A., Whitfield, G. K., and Haussler, M. R. (1996) *J. Biol. Chem. 271*, 5143−5149.
37. Okamura, W. H., Midland, M. M., Hammond, M. W., Abd. Rahman, N., Dormanen, M. C., Nemere, I., and Norman, A. W. (1995) *J. Steroid Biochem. Mol. Biol. 53*, 603−613.
38. Sicinski, R. R., Prahl, J. M., Smith, C. M., and DeLuca, H. F. (1998) *J. Med. Chem. 41*, 4662−4674.
39. Fontana, A. (1972) *Methods Enzymol. 25*, 419−423.
40. Chakraborti, P. K., Garabedian, M. J., Yamamoto, K. R., and Simons, S. S., Jr. (1992) *J. Biol. Chem. 267*, 11366−11373.
41. Wecksler, W. R., Ross, F. P., and Norman, A. W. (1979) *J. Biol. Chem. 254*, 9488−9491.
42. Coty, W. A. (1980) *J. Biol. Chem. 255*, 8035−8037.
43. Pike, J. W. (1981) *Biochem. Biophys. Res. Commun. 100*, 1713−1719.
44. Baker, A. R., McDonnel, D. P., Hughes, M., Crisp, T. M., Mangelsdorf, D. J., Haussler, M. R., Pike, J. W., Shine, J., and O'Malley, B. W. (1988) *Proc. Natl. Acad. Sci. U.S.A. 85*, 3294−3298.
45. Burmester, J. K., Wiese, R. J., Maeda, N., and DeLuca, H. F. (1988) *Proc. Natl. Acad. Sci. U.S.A. 85*, 9499−9502.
46. Elaroussi, M. A., Prahl, J. M., and DeLuca, H. F. (1994) *Proc. Natl. Acad. Sci. U.S.A. 91*, 11596−11600.
47. MacDonald, P. N., Dowd, P. R., and Haussler, M. R. (1994) *Semin. Nephrol. 14*, 101−118.
48. Anstead, G. M., Carlson, K. E., and Katzenellenbogen, J. A. (1997) *Steroids 62*, 268−303.
49. Aliau, S., Garrouj, D. E., Yasri, A., Katzenellenbogen, B. S., and Borgna, J.-L. (1997) *Biochemistry 36*, 5861−5867.
50. Murdock, G. L., Warren, J. C., and Sweet, F. (1988) *Biochemistry 27*, 4452−4458.
51. Swamy N., Brisson M., and Ray R. (1995) *J. Biol. Chem. 270*, 2636−2639.
52. Swamy, N., Kounine, M., and Ray, R. (1996) *J. Bone Min. Res. 11*, Suppl. 1, M545.
53. Norman, A. W., Bishop, J. E., Collins, E. D., Satchell, D. P., Dormanen, M. C., Zanello, S. B., Farcah-Carson, M. C., Bouillon, R., and Okamura, W. H. (1996) *J. Steroid Biochem. Mol. Biol. 56*, 13−22.
54. Ray, R. (1998) in *Vitamin D: Physiology, Molecular Biology and Clinical Applications* (Holick, M. F., Ed.) pp 147−162, Humana Press, NJ.
55. Swamy, N., Dutta, A., and Ray, R. (1997) *Biochemistry 36*, 7432−7436.
56. Swamy, N., Addo, J., Vskokovic, M. R., and Ray, R. (2000) *Arch. Biochem. Biophys. 373*, 471−478.
57. Weatherman, R. V., Fletterick, R. J., and Scanlan, T. S. (1999) *Annu. Rev. Biochem. 68*, 559−581.
58. Väisänen, S., Rouvinen, J., and Mäenpää, P. H. (1998) *FEBS Lett. 440*, 203−207.
59. Rochel, N., Wurtz, J. M., Mitschler, A., Klaholz, B., and Moras, D. (2000) *Mol. Cell 5*, 173−179.
60. Yamamoto, K., Masuno, H., Choi, M., Nakashima, K., Taga, T., Ooizumi, H., Umesono, K., Sicinska, W, Van Hooke, J., DeLuca, H. F., and Yamada, S. (2000) *Proc. Natl. Acad. Sci. U.S.A.*, 1467−1472.

BI0002131